PART A: PRECIPITATION HARDENING IN A TI-CU ALLOY

PART B: THE STRUCTURAL AND MAGNETIC PROPERTIES OF SOME QUARTERNARY ALLOYS OF $Mn_{60}Al_xZn_{20-x}C_{20}$ AND $Mn_{60}Ga_xZn_{20-x}C_{20}$

by

LAWRENCE MARTIN HOWE

A THESIS SUBMITTED IN PARTIAL FULFILMENT OF THE REQUIREMENTS FOR THE DEGREE OF MASTER OF APPLIED SCIENCE

in the Department of MINING AND METALLURGY

We accept this thesis as conforming to the standard required from candidates for the degree of MASTER OF APPLIED SCIENCE.

Members of the Department of Mining and Metallurgy.

THE UNIVERSITY OF BRITISH COLUMBIA

August, 1956

ABSTRACT

The decreasing solid solubility limit at the titanium-rich end of the titanium-copper constitutional diagram suggests the possibility that titanium-rich alloys may be age-hardenable. However, results obtained by previous investigators, using lump samples, show that after quenching from 790°C the age-hardening of an alloy containing 1.7 percent copper is very light while a 0.8 percent copper alloy decreases in hardness, during heat treatment at 400°C.

It was believed possible that powder samples of alloys might show different results from the lump samples used by previous investigators. Consequently, a 1.90 percent copper alloy was made by the technique of levitation melting, checked for homogeneity, and filings of 48-65 Tyler screen size were cut from it for aging experiments.

Hardness readings do show a hardness peak at aging temperatures of 400°C, 450°C, and 500°C and thus indicate that the titanium-copper alloy is susceptible to age-hardening treatments.

Interest in the $Mn_{60}Al_xZn_{20-x}C_{20}$ and $Mn_{60}Ga_xZn_{20-x}C_{20}$ systems results from pregious studies of Mn-Al-C, Mn-Zn-C, and Mn-Ga-C systems; in particular the alloys near compositions $Mn_{60}Al_{20}C_{20}$, $Mn_{60}Zn_{20}C_{20}$, and $Mn_{60}Ga_{20}C_{20}$.

The saturation magnetization (σ) versus temperature (T) curve for alloys near the compositions $Mn_{60}Al_{20}C_{20}$ and $Mn_{60}Ga_{20}C_{20}$ shows normal ferromagnetic behaviour from 0°K to the Curie points of the alloys. Alloys near the composition $Mn_{60}Zn_{20}C_{20}$, on the other hand, have abnormal behaviour as they experience a maximum in the σ-T curve in the neighbourhood of -40°C.

Reasons for investigating the $Mn_{60}Al_xZn_{20-x}C_{20}$ and $Mn_{60}Ga_xZn_{20-x}C_{20}$ systems were:

1. to provide further data regarding the presence of abnormal behaviour in $Mn_{60}Zn_{20}C_{20}$ and of normal behaviour in $Mn_{60}Al_{20}C_{20}$ and $Mn_{60}Ga_{20}C_{20}$. (i.e. alloys near these compositions).

2. to suggest how the valency of the cube-corner atom affects the normal ferromagnetic moment of these alloys.

However, investigation of these systems has lead to even more complicated phenomena and the above two items remain, to a large extent, unsolved.

ACKNOWLEDGEMENT

The author is grateful for financial aid in the form of a research assistanceship provided by the Defence Research Board of Canada.

The precipitation hardening studies in the Ti-Cu alloy were originally started by E. Saaremaa in partial fulfilment of B.A.Sc. requirements. This work is part of a program sponsored by the Defence Research Board of Canada, Project Number 7501-18.

Funds for the magnetic studies were provided by the Defence Research Board under Research Grant 281.

Assays were required for the $Mn_{60}Al_xZn_{20-x}C_{20}$ and $Mn_{60}Ga_xZn_{20-x}C_{20}$ alloys and these were kindly done by the Cosma Testing Laboratories in Cleveland, Ohio.

The author is grateful for the assistance of the staff of the Department of Mining and Metallurgy. Special thanks are extended to Dr. J. Gordon Parr, director of the Ti-Cu research, Dr. H.P. Myers, director of the magnetic research, and R.G. Butters for technical advice and encouragement.

TABLE OF CONTENTS

ILLUSTRATIONS

ILLUSTRATIONS (continued) Page

PART A: PRECIPITATION HARDENING IN A TI-CU ALLOY

I. INTRODUCTION

The necessary condition for carrying out a precipitation hardening process on an alloy is that at room temperature there shall be present in the slowly cooled alloy a large amount of one phase and a smaller amount of a second phase. The first constituent must be capable of dissolving all or an appreciable amount of the second constituent as the temperature is raised.

The decreasing solid solubility limit at the titanium-rich end of the titanium-copper constitutional diagram[1] (Figure 1) suggests the possibility that titanium-rich alloys may be age-hardenable. Referring to Figure 1, we see that at 798°C, copper is soluble in titanium to the extent of 2.1 percent, whereas the solubility is approximately 0.5 percent at room temperature.

Ordinarily, concentrations of the hardening constituent approaching maximum solid solubility in the α phase at the eutectoid temperature are chosen. The first step in the heat treatment is to heat the alloy to a temperature in the α phase field in order to obtain a solid solution of uniform composition. The saturated solution thus formed is quenched or at least cooled at too rapid a rate to permit the separation of the second phase that would normally occur with slow cooling.

As a result of the rapid cooling, the alloy is in a state of supersaturation and is therefore thermodynamically unstable. The subsequent age-hardening of the alloy is a result of the decomposition of the solution, which in some alloys occurs at ordinary room temperatures but usually requires a relatively low temperature heat treatment.

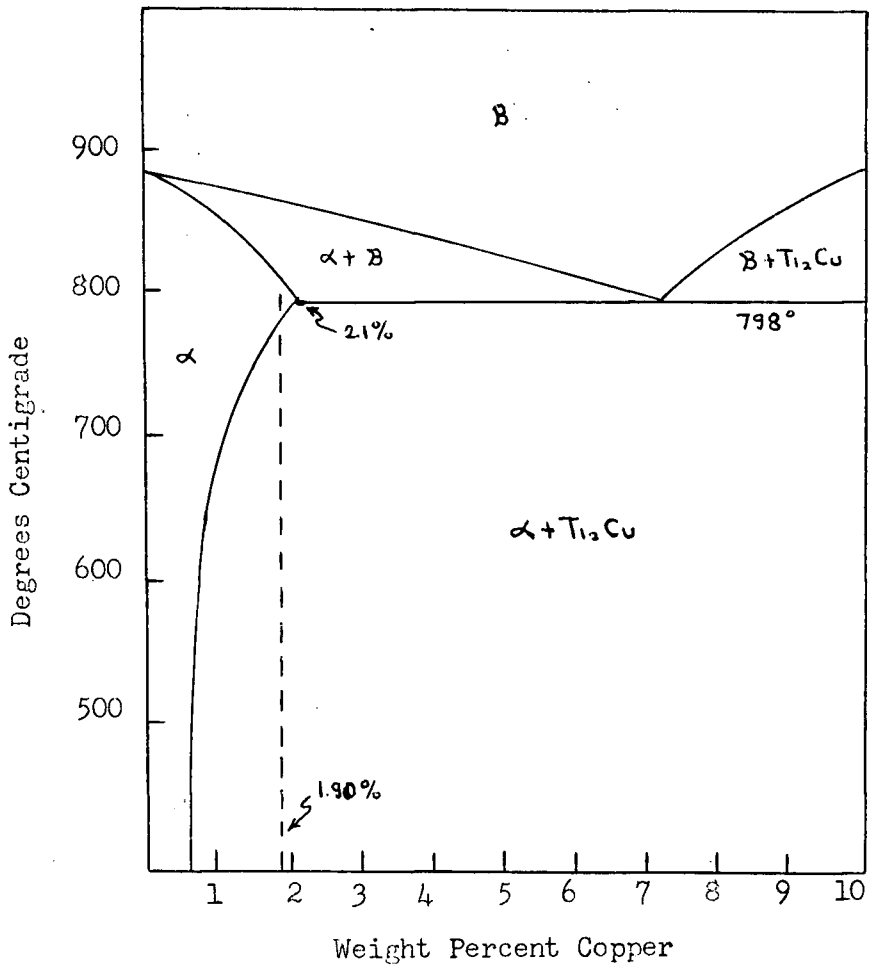

Figure 1 α solid solubility and cutectoid region on the high titanium side of the Ti-Cu phase diagram.

II PREVIOUS WORK

Results obtained by Holden et al[2] reproduced in Figure 2 show that after quenching from 790°C the age-hardening of an alloy containing 1.7 percent copper is very slight, while a 0.8 percent alloy decreases in hardness, during heat treatment at 400°C.

However Holden et al used lump samples and it was believed possible that powder samples of alloys might show different results from the lump samples. Reason for believing thusly is that small particles are often more sensitive to diffusion processes than larger samples.

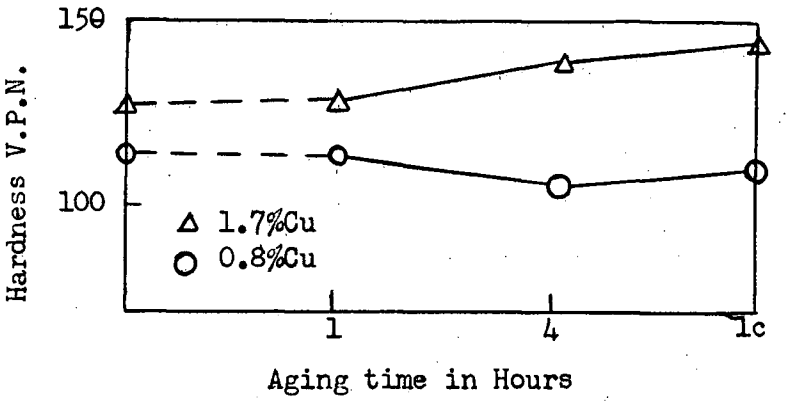

Figure 2 Effect of 400°C aging on hardness of Ti-Cu alloys solution annealed in the α field as determined by Holden, Watts, Ogden, and Jaffee.

III. EXPERIMENTAL PROCEDURE

Preparation of the Alloys.

Owing to the high melting-point of titanium (1800°C) difficulties are encountered in melting techniques. Method adapted was that of melting the titanium alloy by levitation[3] in a high-frequency field.

Initial preparation involved placing the required amount of copper (1.90 percent by weight) in a hole drilled in a cylindrical iodide titanium sample. Weight of the prepared specimen was approximately 6 grams.

The titanium-copper specimen was melted in about 30 seconds and it remained levitated, without dripping, in the molten state in an argon atmosphere (Figure 3). When the coil current is switched off the metal drops into a copper mold directly below the coil. A typical ingot is shown in Figure 4.

There was no trace of reaction or sintering between the mold and the alloy. The ingots were shown to be homogeneous both by microscopic examination and by the identical X-ray diffraction patterns which were obtained from similarly treated samples of different parts of the same ingot.

Previous investigators in the department had done checks on contamination. A piece of pure iodide titanium was melted, cast, and hardness readings were taken. The readings varied from R_F 80 at the center to 90 at the outside. (usual hardness value quoted for pure as-cast titanium is 70 to 75 R_F). The ingot was melted a second and a third time and there was no change in these hardness values. Therefore, according to accepted standards, there was no contamination during melting.

Heat Treatments.

A gas-quenching furnace was used for quenching operations. Filings of 48-65 Tyler screen size were cut from the ingot and placed in a small molybdenum boat. The boat and the sample were than placed in a furnace, held in an atmosphere of argon while heated to 790°C for several minutes, and then blown out of the heating zone into a flask by a jet of helium gas. No reaction occurred between the filings and the boat and the filings did not appear to be sintered.

For aging, the filings were sealed in vacuo in silica tubes and aged at temperatures of 400°C, 450°C, and 500°C for various time intervals.

Microhardness Measurements.

Hardness readings were taken on a Bergsman Microhardness Tester, using a 25 gram load applied to a diamond indenter. Filings were mounted in lucite for this test.

Figure 3 Photograph of levitation-melting unit in operation.

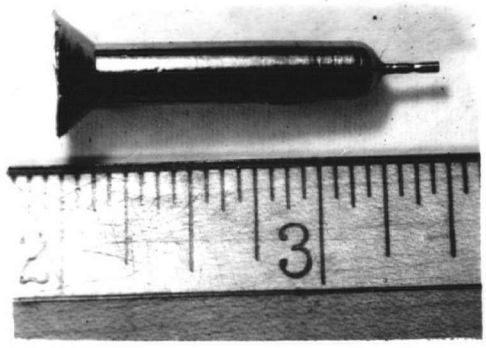

Figure 4 Photograph of typical titanium alloy ingot.

IV. RESULTS

Hardness readings taken at various time intervals for aging temperatures of 400°C, 450°C, and 500°C are plotted in Figure 5. From this graph it is seen that a hardness peak is obtained at each aging temperature.

About a dozen readings were taken on each heat-treatment sample; the highest reading and the lowest reading were ignored and an average taken of the remaining values. In Figure 5 the curves pass through the average readings while the extent of scatter is shown by the length of the vertical lines drawn through each point on the curves.

Microstructures of all samples were examined and X-ray goniometer plots were taken between 2θ values of 34° and 44° for as quenched, age-hardened 10 minutes, and age-hardened 1000 minutes samples for all three aging temperatures. Microstructures showed the presence of α only and likewise X-ray goniometer plots only revealed the presence of close-packed hexagonal α lines namely: 100 at 35°, 002 at 38.2°, and 101 at 40.1°. No lines at 39.5° and 43° characteristic of Ti_2Cu were present. (above angles are 2θ values).

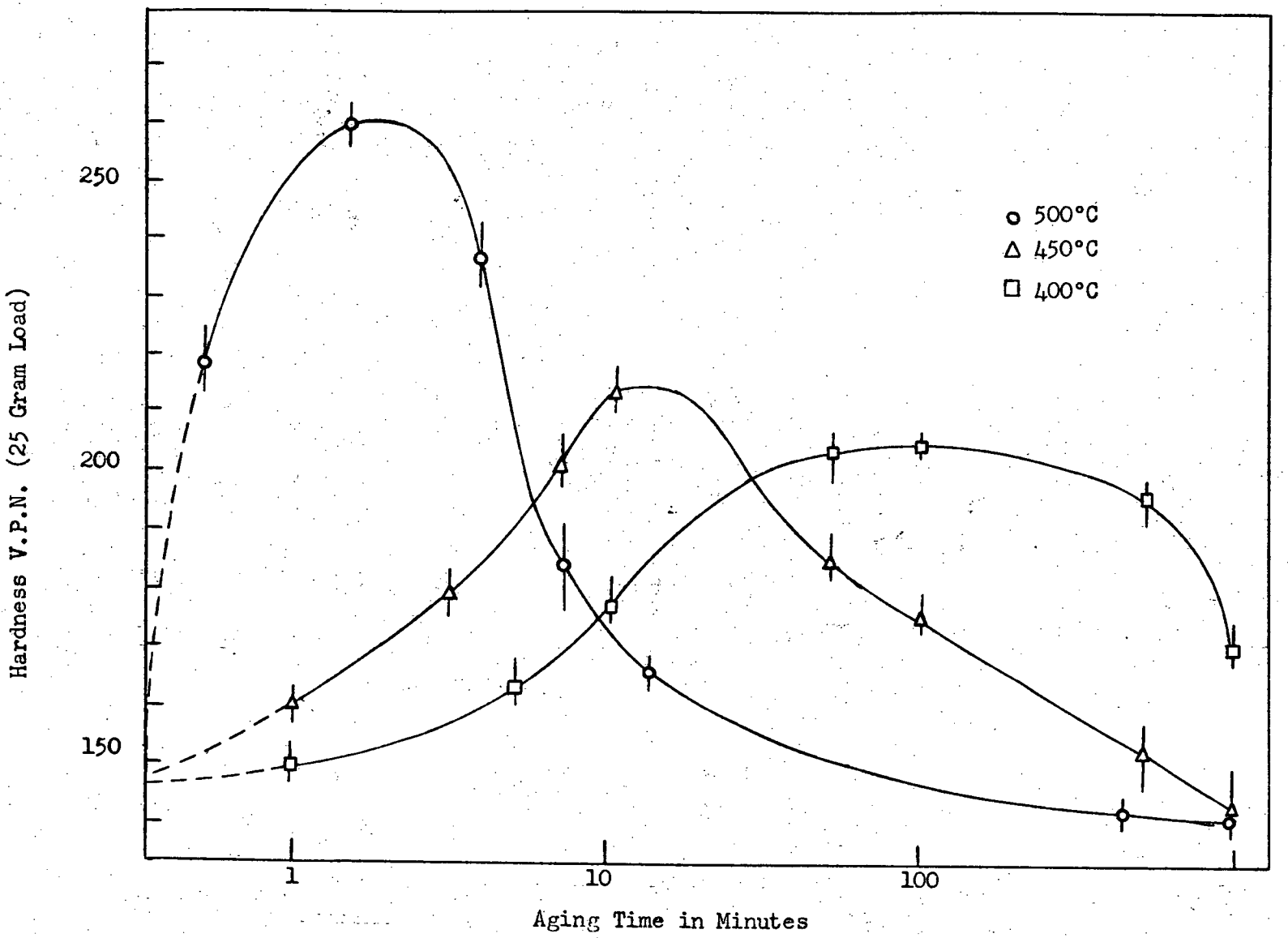

Figure 5 Effect of 400°C, 450°C, 500°C aging on hardness of 1.90%Cu alloy, in powder form, as determined by author.

V. DISCUSSION OF RESULTS AND CONCLUSIONS

Microscopic and X-ray examinations failed to reveal any structural changes during the aging process. This is not too surprising since early stages of precipitation do not usually manifest themselves in ways that are readily detectable by metallographic methods and the extent of precipitation on overaging a 1.90 percent copper alloy is very small.

It is generally accepted that during aging some hardening occurs as a result of stresses set up by 'pre-precipitation' processes. At low temperatures of aging actual precipitation never occurs and hence the hardness curve is asymptotic to a line parallel to the time axis. At higher temperatures of aging precipitation occurs, stresses are relieved, and the hardness curves fall off.

In the titanium-copper alloy at temperatures between 400°C and 500°C the hardness curves show characteristics that are typical of overaging. Experiments conducted at lower temperatures by other investigators, also using powdered samples, gave no positive indication of hardness increase. Therefore, it appears that the coherency between the precipitate and the matrix material is short lived at the temperatures investigated - a fact which may be peculiar to the titanium-copper system or to the use of samples of very small dimensions.

Quite apart from this 'overaging' preculiarity, the results indicate that the titanium-copper specimens are readily susceptible to age hardening treatments. †This is in contrast with the behaviour of lump samples which are reported by other workers [2] to respond negligibly.

VI. BIBLIOGRAPHY

1. A Joukainen, N.J. Grant, C.F. Floe, Trans A.I.M.E. (1952), 194, 766.
2. F.C. Holden, A.A. Watts, H.R. Ogden, R.I. Jaffee, Trans A.I.M.E. (1955), 203, 117.
3. D.H. Polonis, R.G. Butters, J.G. Parr, Research (1954), 7, 10s.
4. D.H. Polonis, J.G. Parr, Trans A.I.M.E. (1954), 200, 1148.

PART B: THE STRUCTURAL AND MAGNETIC PROPERTIES OF SOME QUATERNARY ALLOYS OF $Mn_{60}Al_xZn_{20-x}C_{20}$ AND $Mn_{60}Ga_xZn_{20-x}C_{20}$

I. INTRODUCTION

Weiss[1], in his molecular field approach to magnetism, obtains the following relationship for ferromagnetics:

$$\sigma_s/\sigma_o = \tanh(\sigma_s\theta/\sigma_o T)$$

Where σ_s is the saturation magnetization at temperature in question, σ_o is the saturation magnetization at absolute zero, T is the temperature, and θ is the Curie point defined by:

$$\theta = \mu N \sigma_o / K$$

Where μ is the atomic or molecular magnetic moment, K is Boltzmann's universal gas constant, and N is the Weiss intermolecular field constant.

In the above, Weiss is using the assumption of quantum theory namely that there are only two directions permissible for the spins of the elections ie: parallel and antiparallel.

The general relationship between saturation magnetization and

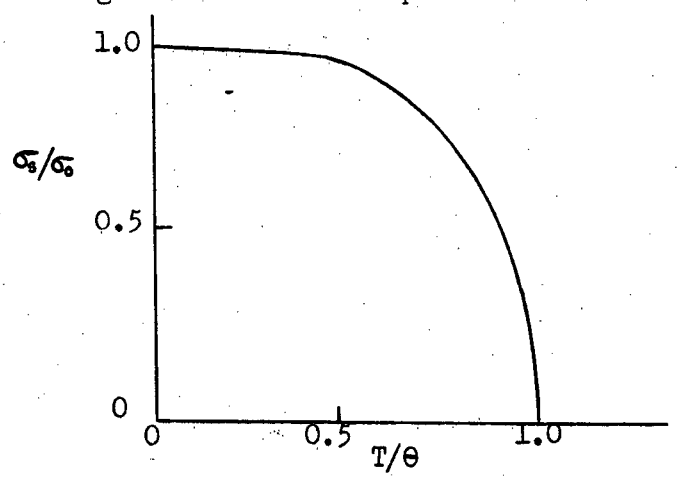

Figure 1 General relation between saturation value and temperature for ferromagnetics.

temperature which is listed above is plotted in Figure 1.

The experimentally observed saturation value of the ferromagnetics does in fact fall with rising temperature reaching substanitally zero at a temperature known as the Curie temperature or magnetic change point. The observed relations for the elements iron, cobalt, and nickel are in good agreement with the above theory.

A plot of saturation value (σ_s) versus temperature (T) for alloys near the compositions $Mn_{60}Al_{20}C_{20}$ and $Mn_{60}Ga_{20}C_{20}$ indicate that these alloys obey normal ferromagnetic behaviour from absolute zero to the Curie points. However, alloys near the composition $Mn_{60}Zn_{20}C_{20}$ do not exhibit normal ferromagnetic behaviour as a maximum occurs in the σ -T curve at approximately -40°C.

In order to obtain further information with regard to this abnormal behaviour , it was desirable to investigate the magnetic properties of the systems $Mn_{60}Al_xZn_{20-x}C_{20}$ and $Mn_{60}Ga_xZn_{20-x}C_{20}$.

Alloys of the compositions $Mn_{60}Al_{20}C_{20}$, $Mn_{60}Ga_{20}C_{20}$ and $Mn_{60}Zn_{20}C_{20}$ have a highly-ordered structure in which manganese occupies face-center positions of cube, carbon occupies the body-center position, and aluminum, gallium, or zinc atoms are at the cube corners. The proposed structure appears in Figure 2.

Through an investigation of $Mn_{60}Al_xZn_{20-x}C_{20}$ and $Mn_{60}Ga_xZn_{20-x}C_{20}$ systems, it was thus also desired that information could be obtained which would suggest how the valency of the cube-corner atom affects the normal ferromagnetic moment of these alloys.

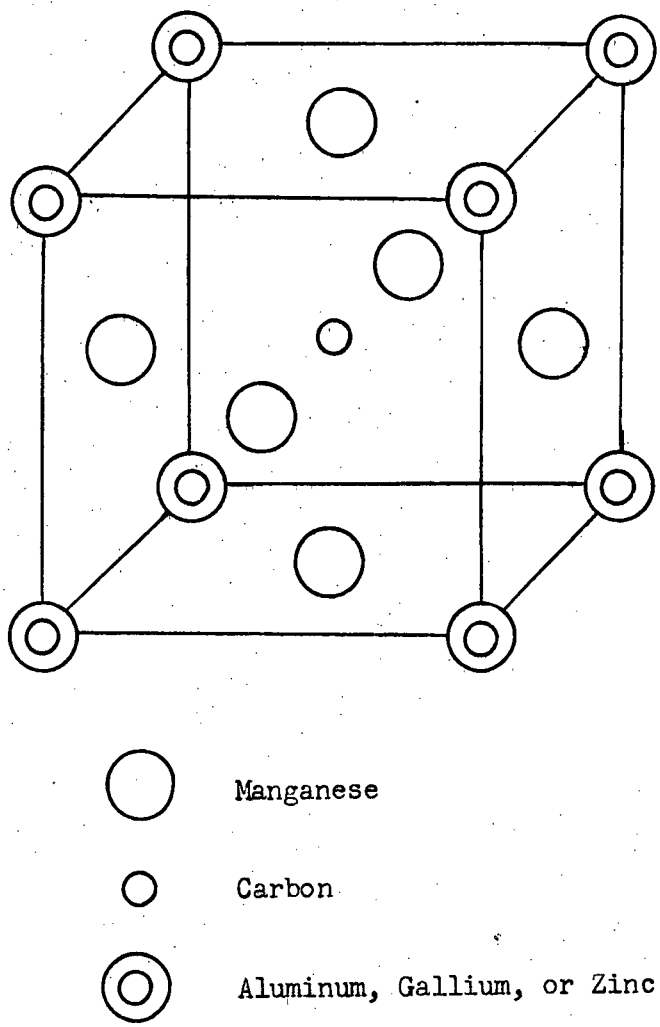

Figure 2 The proposed structure of $Mn_{60}Al_{20}C_{20}$, $Mn_{60}Ga_{20}C_{20}$, and $Mn_{60}Zn_{20}C_{20}$.

II. PREVIOUS WORK

Mn-Al-C System

Butters and Myers[2] investigated alloys close to the composition $Mn_{60}Al_{20}C_{20}$. For a fixed carbon content of 20 atomic percent the single face-centered cubic structure occurs over the composition range Mn 60-69 atomic percent (hence Al 20-11 atomic percent).

Increasing the manganese content beyond 60 atomic percent to 70 atomic percent causes an increase in the Curie temperature from 0°C to 300°C, a decrease in the saturation magnetization from 1.20 to approximately 0.6 Bohr magnetons per manganese atom, and a slight increase in the lattice paramater from 3.869A° to 3.874A°. This decrease in magnetization as the manganese content is increased past 60 atomic percent can be explained by assuming that the magnetization of the additional manganese atoms, which must replace aluminum atoms in cube corner positions, is antiparallel to that of those in the face-centered positions. The magnitude of the decrease in magnetization corresponds to the extra manganese atoms having an effective Bohr magneton value of -4.

In these alloys the saturation magnetization below the Curie temperature varies with temperature in a normal ferromagnetic manner as can be seen in Figure 3 for an alloy near the composition $Mn_{60}Al_{20}C_{20}$. Paramagnetic behaviour above the Curie point seems to indicate ferrimagnetism, however neutron diffraction results indicate that $Mn_{60}Al_{20}C_{20}$ is ferromagnetic.

Mn-Zn-C System

Butters and Myers[3] also investigated the behaviour of alloys near the composition $Mn_{60}Zn_{20}C_{20}$. Within the range of composition studied, C 20 atomic percent, Zn 10-20 atomic percent, Mn 70-60 atomic percent, it was found that the structure of the alloys was face-centered cubic. Increasing the manganese content beyond 60 atomic percent to 70 atomic percent causes an increase in the Curie point from 80° to 488°C and a decrease of the lattice parameter from 3.925A° to 3.899A°.

For alloys with a zinc content above 15 atomic percent a marked maximum in the magnetization occurs in the region of -40°C to -50°C. Above this temperature the magnetization decreases in the usual fashion becoming zero at the Curie point. Below this temperature region the magnetization decreases but the decrease becomes less the lower the temperature. This abnormal behaviour for an alloy near composition $Mn_{60}Zn_{20}C_{20}$ is shown in Figure 3. Also, for this alloy, it was found that at -186°C the original face-centered cubic structure observed at room temperatures is slightly distorted becoming face-centered tetragonal with a=3.921A° and c/a=0.9947.

Néel[4] has shown that the magnetization of a ferrimagnetic substance may vary with temperature in a similar manner to the abnormal behaviour observed in above Mn-Zn-C alloys. Paramagnetic behaviour above the Curie point also appears to agree with that predicted by Néel for ferrimagnetics.

However, results obtained by Dr. B. Brockhouse at Chalk River, using neutron diffraction techniques, seem to suggest a different magnetic concept. The concept proposed is that of opposing sublattices having different Curie points (the sublattices of a ferrimagnetic substance have the same Curie points).

The Curie point of one sublattice is assumed to be -40°C, where the maximum in the saturation magnetization of $Mn_{60}Zn_{20}C_{20}$ occurs. The other Curie point is at 100°C as observed by magnetic measurements. The resultant magnetization is a vector sum of the opposing sublattices.

It is also rather interesting to note that a second order specific heat anomaly corresponding to the Curie point of one sublattice should occur at -40°C. Such an anomaly has been found to exist in measurements on $Mn_{60}Ga_{20}C_{20}$ by M. Swanson, here at the department.

Mn-Ga-C System

Butters and Myers started this study and the project was then continued by the author. X-ray Debeye-Scherrer diffraction photographs show that, within range of composition, C 20 atomic percent, Mn 62-70 atomic percent, Ga 10-18 atomic percent, the alloys have a face-centered cubic structure. It was not possible to obtain an alloy of composition $Mn_{60}Ga_{20}C_{20}$ as made up alloys of this composition contained free carbon.

Saturation magnetization variation with temperature for alloys indicated normal ferromagnetic behaviour such as that illustrated in Figure 3 for an 18 atomic percent gallium alloy. The lattice parameter increases with increasing manganese content from 3.876A° at 62 atomic percent manganese to 3.881A°, whereas the Bohr magneton value per manganese atom decreases from a value of 1.27 at 62 atomic percent manganese to 0.62 at 70 atomic percent manganese.

This would seem to suggest that the additional manganese atoms (in excess of 60 atomic percent) are replacing the gallium atoms at the cube corners and the magnetization of the cube corner manganese atoms

is antiparallel to that of those in face-centered positions. The magnitude of the decrease corresponds to a value of -4 Bohr magnetons for the extra manganese atoms.

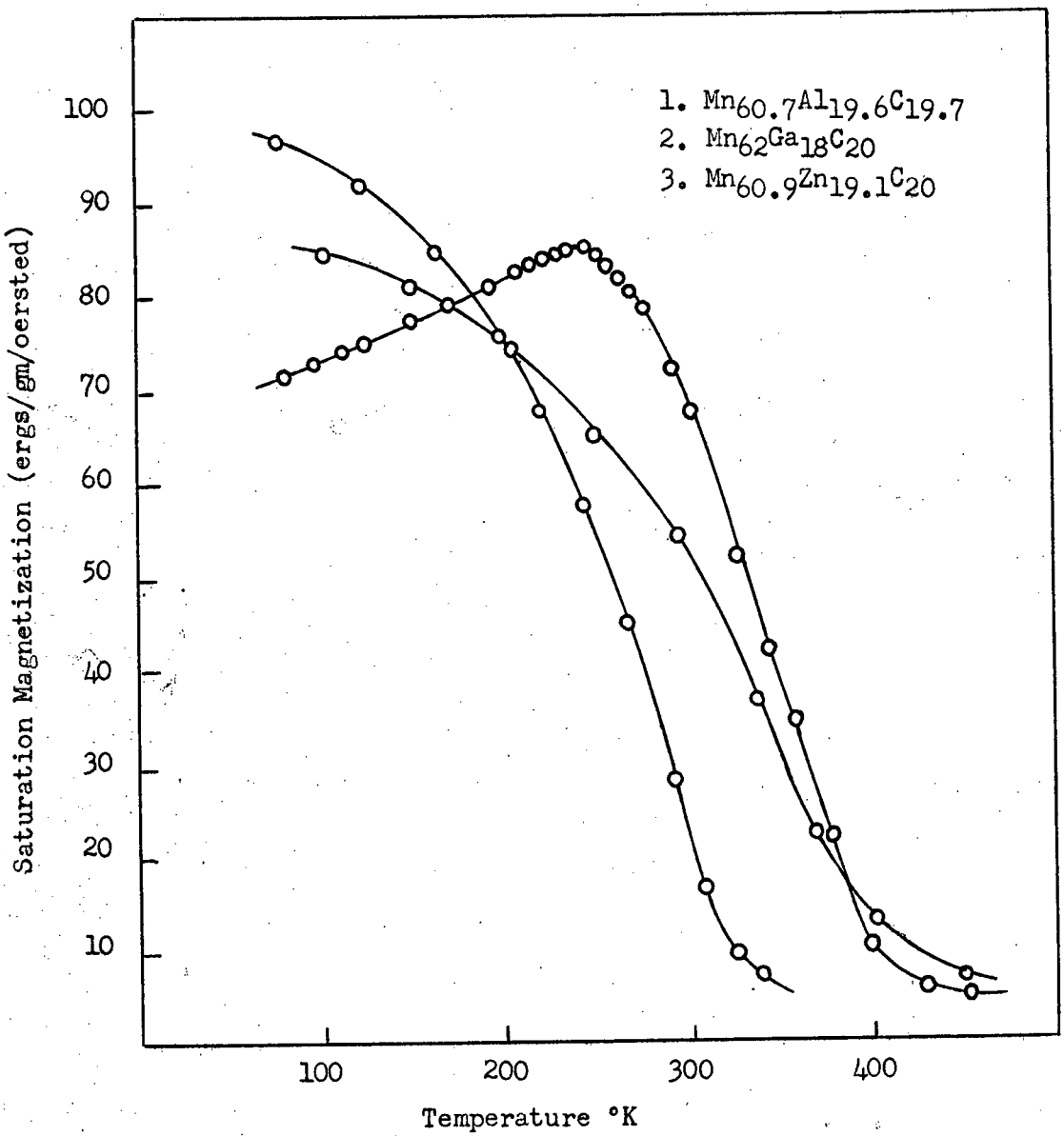

Figure 3 Saturation magnetization versus temperature for alloys near the compositions $Mn_{60}Al_{20}C_{20}$, $Mn_{60}Ga_{20}C_{20}$, and $Mn_{60}Zn_{20}C_{20}$.

III. EXPERIMENTAL PROCEDURE

Preparation of Alloys

The materials used in the preparation of the alloys for this work were manganese of 99.9 percent purity, zinc of 99.99 percent purity, aluminum of 99.99 percent purity, gallium of 99.99 percent purity and graphite of spectroscopic grade.

The first step in the preparation of the alloys was to make Mn-Al-C and Mn-Ga-C master alloys. Melting was carried out by the process of induction heating under an atomosphere of argon after initial evacuation and degassing. Melts were chill cast under argon into a split brass mold. Ingots were annealed in vacua in quartz tubes to remove coring and promote homogeneity. Zinc could not be included in this melting stage due to its low distillation temperature.

Master alloys were then crushed and mixed with the appropriate amount of zinc filings to produce the mixture for sintering. The mixture of powders was placed in a clean fused quartz tube, the tube was evacuated and sealed, and the sintering was achieved by heating to 600°C for approximately one week. In some cases the alloys were recrushed and resintered.

The sinters wer homogeneous but tended to decompose if left in moist air for long periods. They were therefore kept in a dessicator when not in use.

Magnetic Measurements

For the magnetic measurements an external field of 16,200 oersteds was used. The field was obtained by means of an electromagnet having its poles shaped so that a uniform field gradient was produced over a volume considerably greater than that of the specimen.

A Sucksmith ring balance was used to measure the magnetization. The principal involves the comparison of the forces exerted in turn on a sample of alloy and a sample of iron under identical conditions. The magnetic properties of pure iron being accurately known, those of the alloy sample may be calculated.

The alloy specimen experiences a force F_X given by:

$$F_x = \sigma_x m_x dH/dx$$

where σ is the saturation magnetization, m is the mass, and dH/dx is the field gradient.

Under identical conditions an iron standard experiences a force:

$$F_s = \sigma_s m_s dH/dx$$

The forces F_X and F_S are balanced by the restoring force of a beryllium copper ring and the displacement of the specimen is measured by a displaced light beam passing through two mirrors attached to the ring. We thus obtain:

$$K d_x = F_x = \sigma_x m_x dH/dx$$
$$K d_s = F_s = \sigma_s m_s dH/dx$$

from which:

$$\sigma_x = \sigma_s m_s/m_x \; d_x/d_s$$

About 30-40 mg. of sintered alloy was used for measurement, this being placed in a platinum-iridium container. A furnace and dewar attachments permitted measurements over temperature range required namely between -190°C and Curie points (highest about 230°C).

Paramagnetic measurements were not made as there would have been trouble arising due to the distilling out of zinc at elevated temperatures.

X-ray Measurements and Microscopic Examination

Debeye-Sherrer powder photographs were taken and the lattice paramaters were calculated from these in the usual way. Low temperature X-ray intensity plots were made on alloys of high zinc content in

$Mn_{60}Al_xZn_{20-x}C_{20}$ system using a Geiger counter spectrometer.

Samples were mounted in lucite, polished, etched with 4 percent nitol solution, and observed under the microscope. This examination served as an additional check as to whether the alloys were single phase or not.

IV. RESULTS

$Mn_{60}Al_xZn_{20-x}C_{20}$ System

In Figures 4 and 5 the variation of saturation magnetization (σ) with temperature (T) is shown for single phase alloys. Normal ferromagnetic behaviour is experienced by single phase alloys of aluminum content of approximately 5.5 atomic percent and up. Alloys with lower aluminum contents than 5.5 atomic percent have a maximum or very flat portion in their saturation magnetization curves. An alloy consisting of 9.6 atomic percent aluminum was also studied and was found to have normal ferromagnetic behaviour but is not included on the graphs for sake of clarity.

The point at which deviation from normal ferromagnetic behaviour occurs shall be referred to as the transition point, transition temperature or simply transition. The transition temperatures for 0, 2.85, and 4.6 atomic percent aluminum alloys are 231 ± 2, 210 ± 5, and 120 ± 10°K respectively.

In Figure 6 the saturation magnetization at 0°K (σ_o) is plotted against atomic percent aluminum. Normal ferromagnetic alloys are represented by only one point namely σ_o-ordinary which was obtained by an extrapolation of the σ-T curve. Alloys which do not have normal ferromagnetic behaviour are represented by two points namely σ_o-ordinary and σ_o-extraordinary. The first of these represents an extrapolation of the σ-T curve (to absolute zero) above the transition temperature i.e. region characteristic of a normal ferromagnetic. σ_o extra-orindary represents an extrapolation of the σ-T curve below the transition temperature. Vertical and horizontal

lines through the points represent the deviations to be expected in the σ-T extrapolations and in the aluminum compositions. Single phase alloys were not obtainable between 10 and 16 atomic percent aluminum and the dotted line represent form of curve expected if they were obtainable.

The Bohr magneton values have been calculated and then plotted versus atomic percent aluminum. Even though deviations are not shown it is to be understood that they are still applicable. Curve is shown in Figure 7.

Curie temperatures were obtained from σ^2 versus T curves and are plotted versus aluminum content in Figure 8. The variation of Curie temperature with composition certainly is of a rather complex form and since probably very little is to be gained from a study of same it shall not be discussed further.

X-ray Debeye-Sherrer powder photographs show lines characteristic of a face-centered cubic and also superlattice lines. Lattice parameters for single phase alloys decrease linearly from $Mn_{60}Zn_{20}C_{20}$ to $Mn_{60}Al_{20}C_{20}$ as can be seen from Figure 9. Dotted region of curve is that in which single phase alloys were not obtainable.

X-ray line intensity plots were obtained at -186°C and 20°C for alloys of 2.85, 5.5, and 7.5 atomic percent aluminum. Photographs of results for a 2.85 percent alloy are shown in Figure 10. From an examination of the photographs it is noted that there is a definite broadening of 220 and 311 lines at -186°C whereas the 111 line remains unchanged. It appears that 220 and 311 lines are splitting into two components at -186°C but this is not too well resolved. Results for the 5.5 and 7.5 percent alloys are not displayed but it was found that the intensity plots gave no indication of splitting or broadening of lines occurring.

Let us consider for a moment the transition from a cubic to a tetragonal structure. Upon examination of the structures in question it can be seen that as a structure changes from cubic to tetragonal one expects no splitting of X-ray lines for 111 and 222 planes. On the other hand one expects splitting of lines for 200, 220, 311, and 400 planes into two components with multiplicity factors of 2:1.

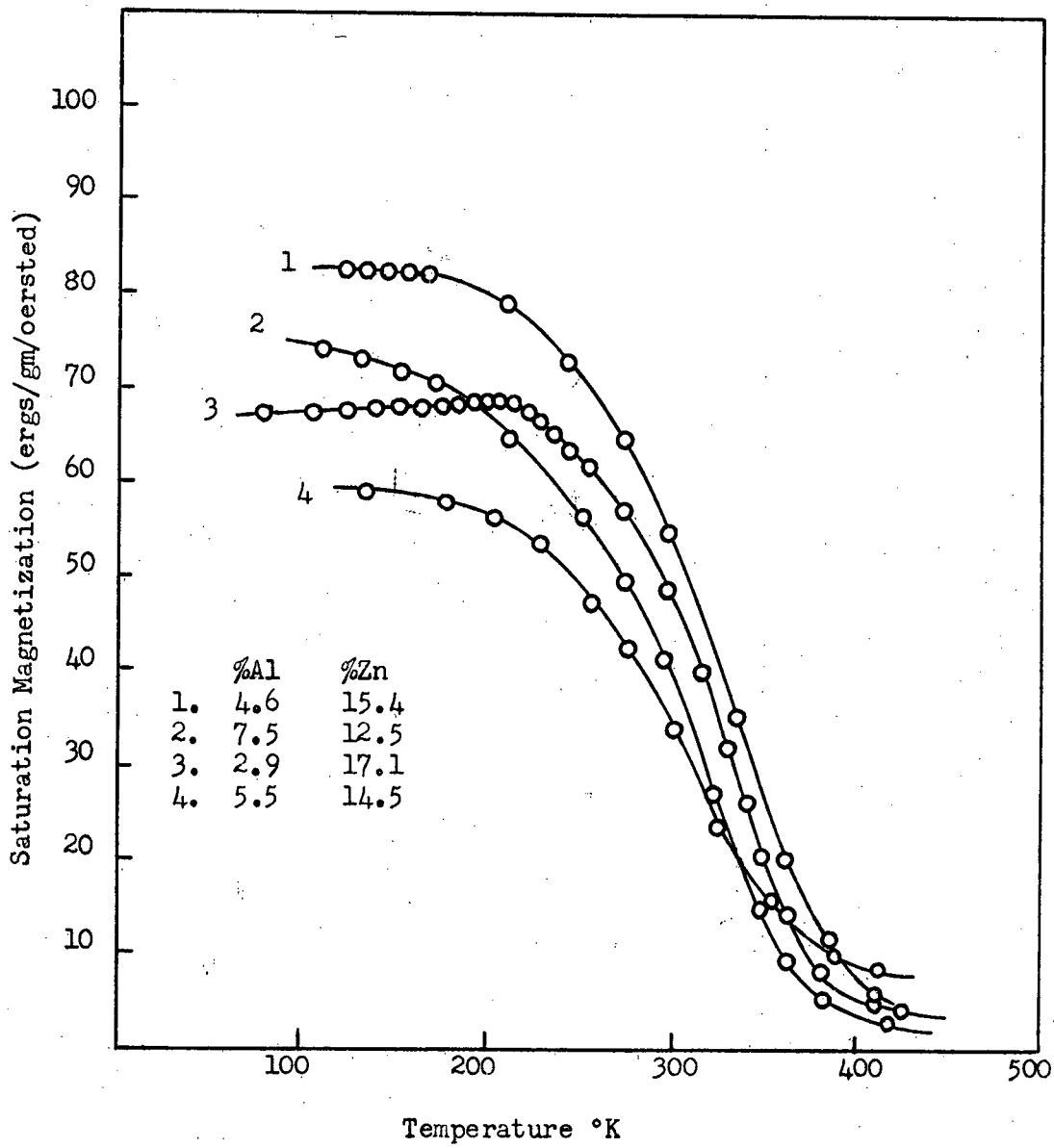

Figure 4 Variation of saturation magnetization with temperature for high zinc content alloys in the $Mn_{60}Al_xZn_{20-x}C_{20}$ system.

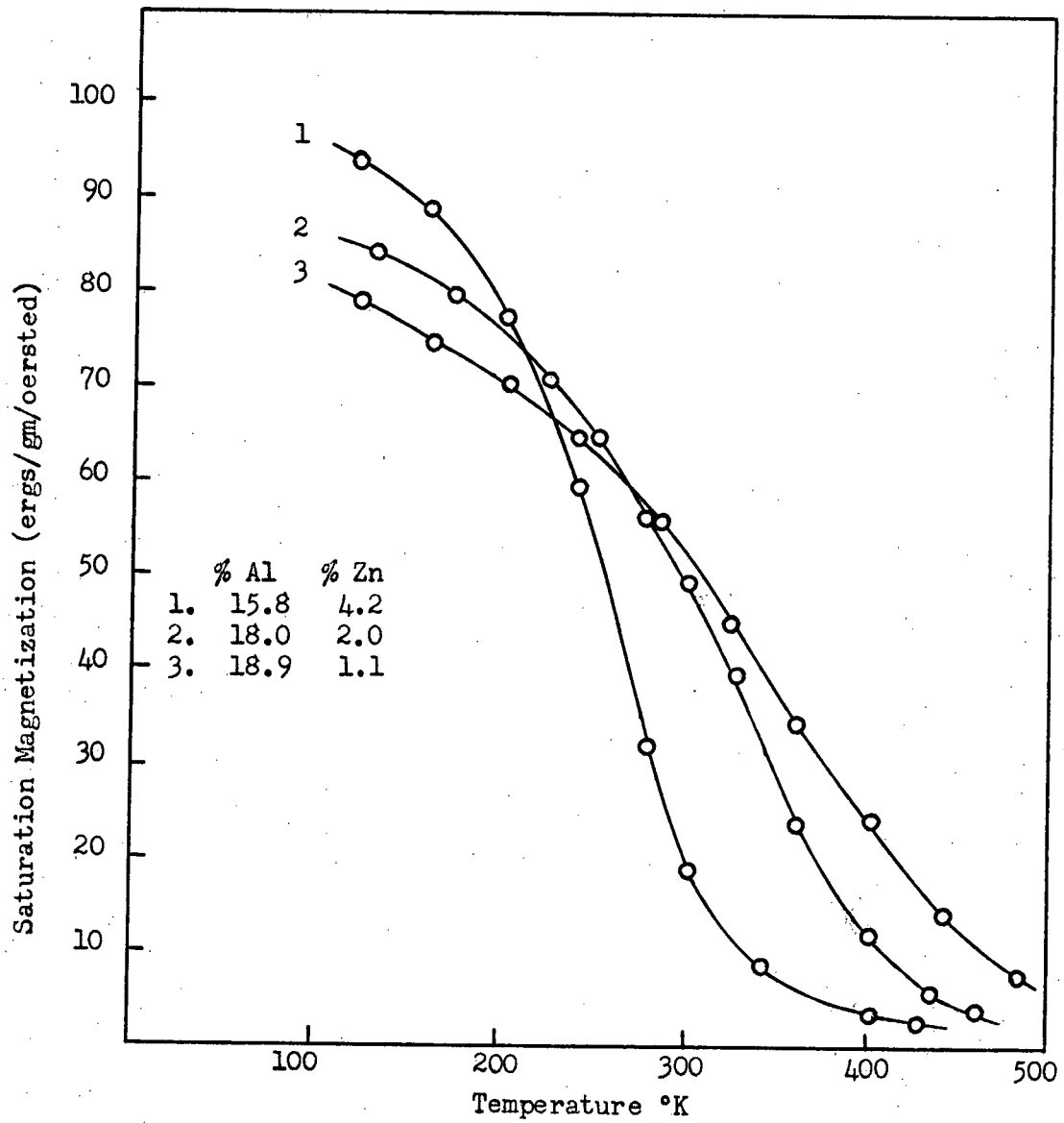

Figure 5 Variation of saturation magnetization with temperature for high aluminum content alloys in the $Mn_{60}Al_xZn_{20-x}C_{20}$ system.

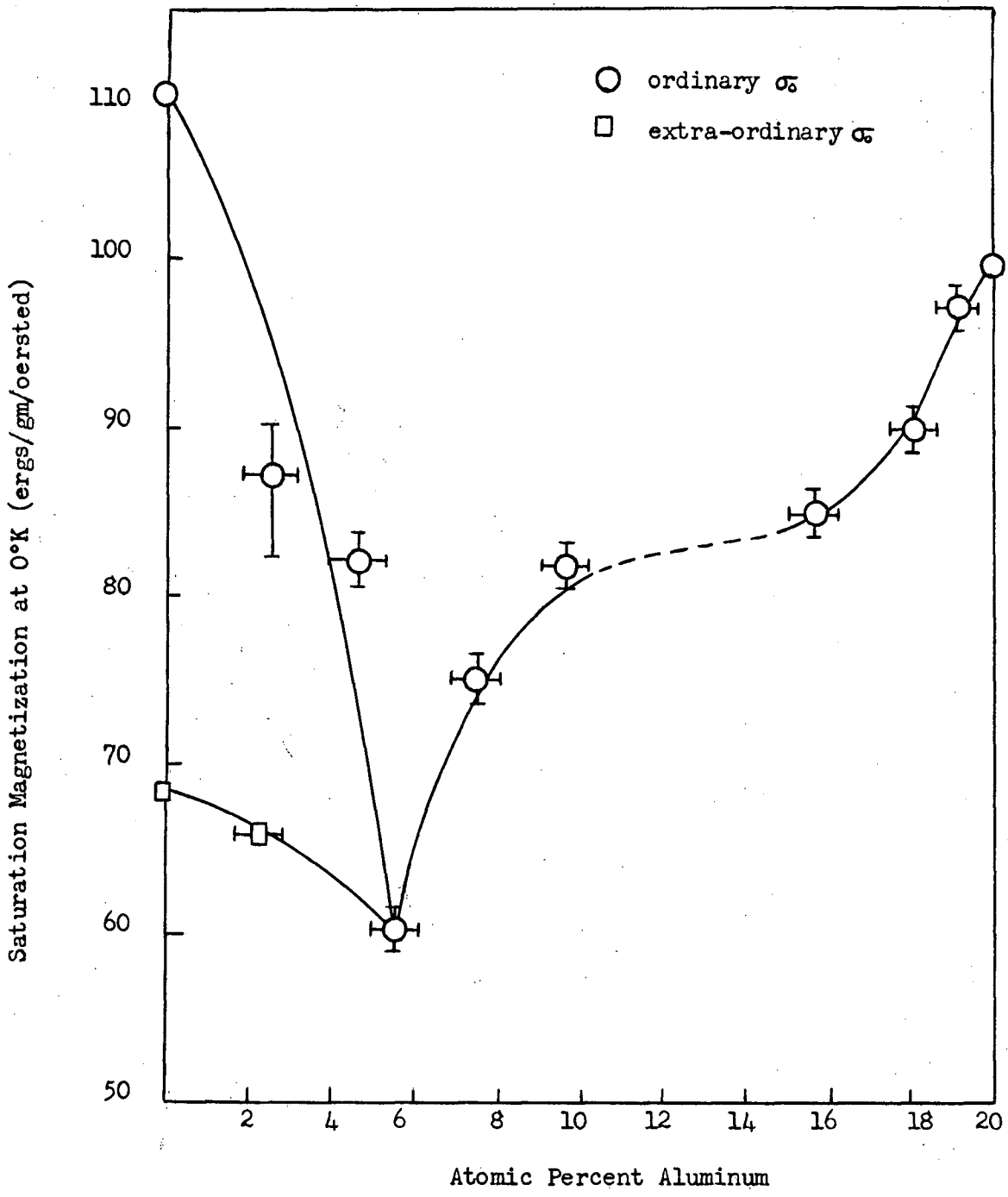

Figure 6 Variation of saturation magnetization at 0°K with atomic percent aluminum for the $Mn_{60}Al_xZn_{20-x}C_{20}$ system.

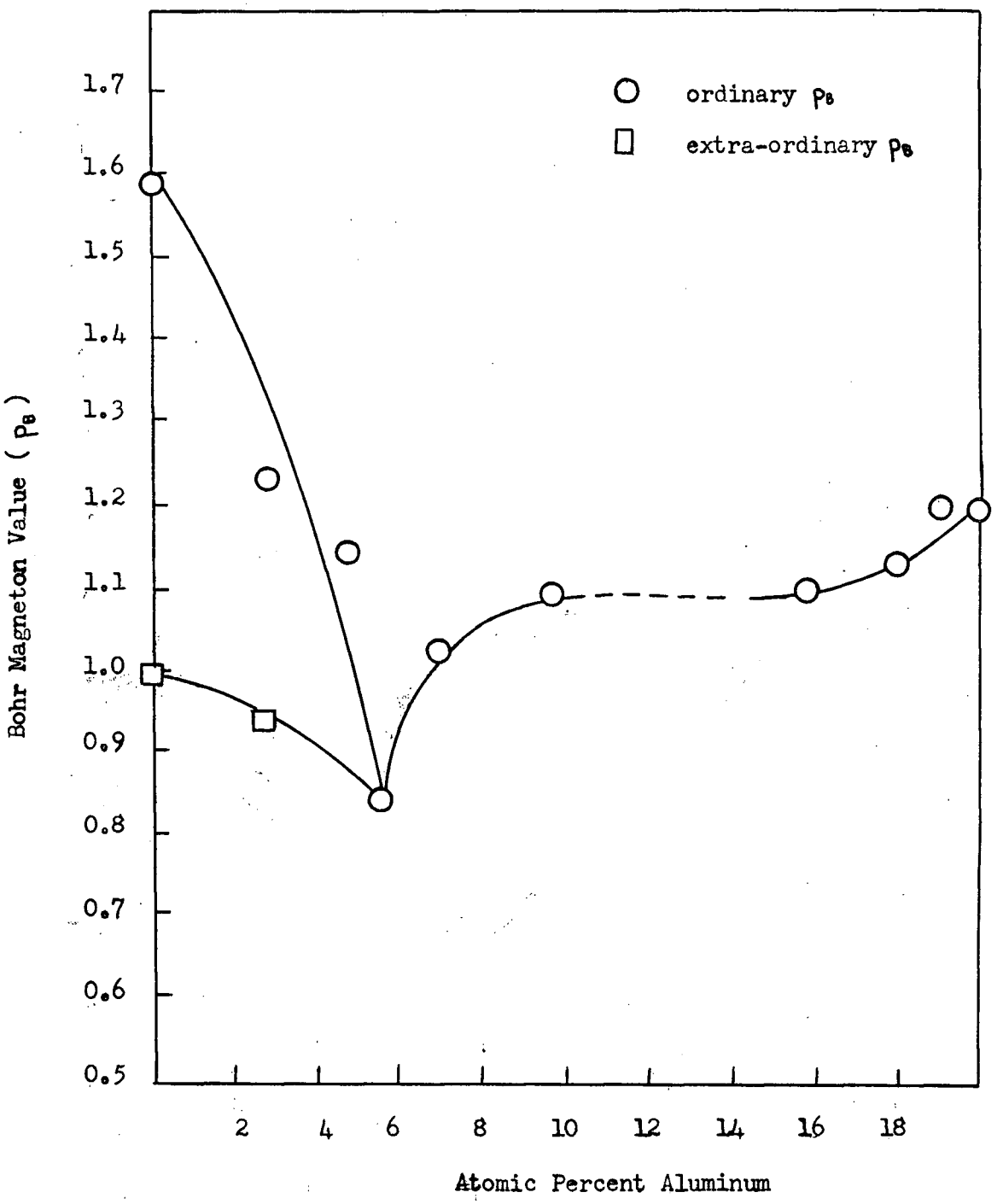

Figure 7 Bohr magneton value versus atomic percent aluminum for the $Mn_{60}Al_xZn_{20-x}C_{20}$ system.

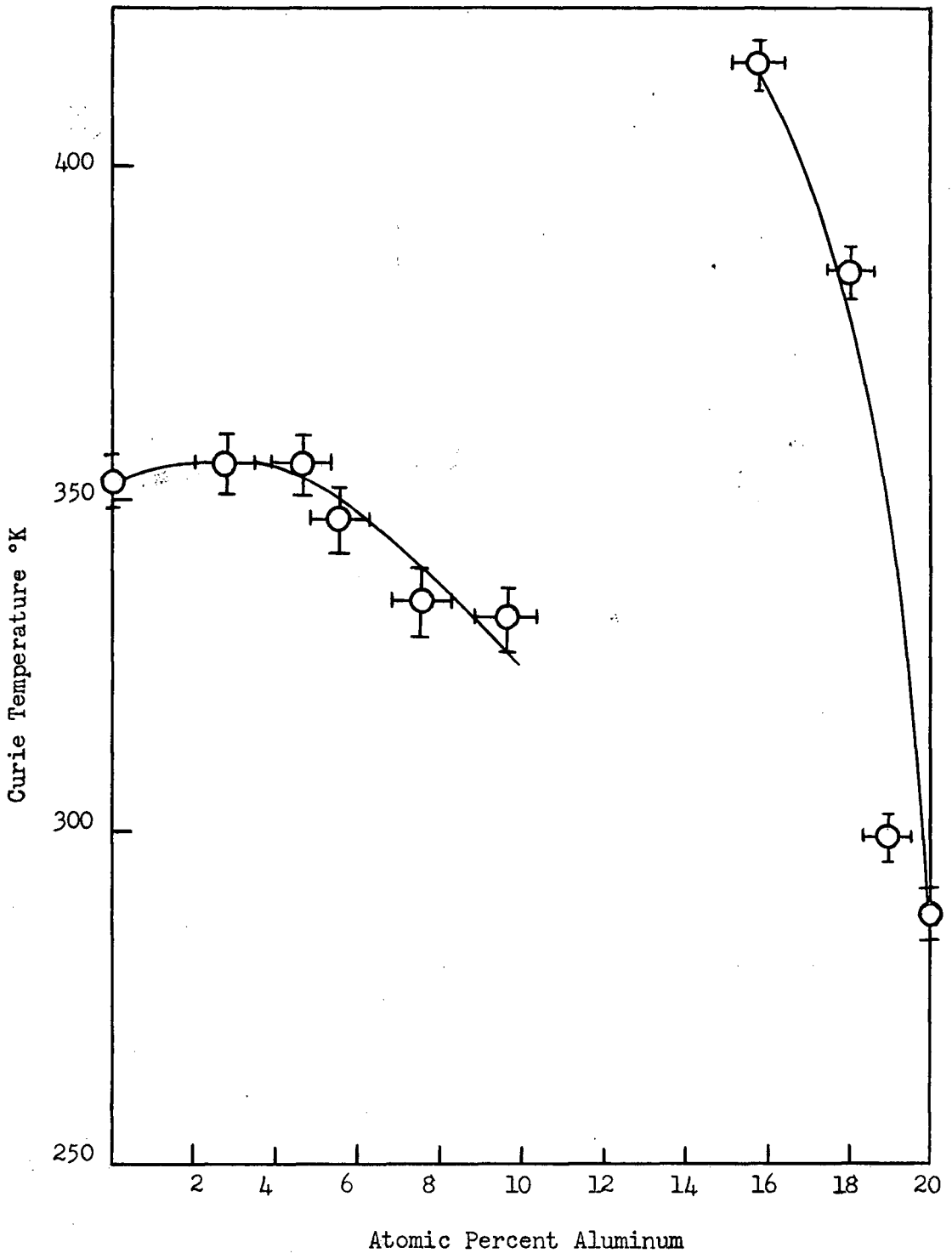

Figure 8 Variation of Curie temperature with atomic per cent aluminum in the $Mn_{60}Al_xZn_{20-x}C_{20}$ system.

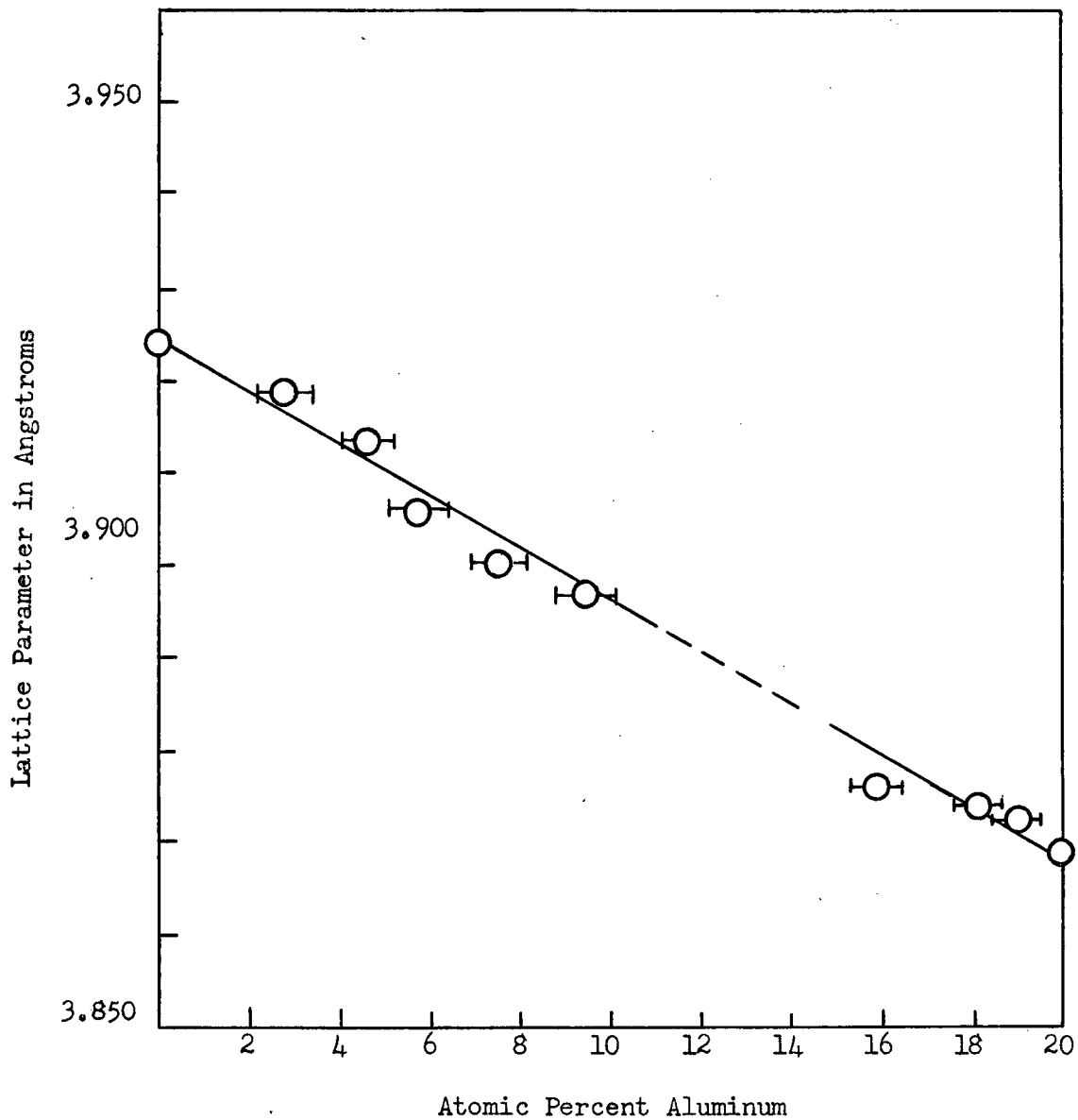

Figure 9 The variation of lattice parameter with atomic percent aluminum for the $Mn_{60}Al_xZn_{20-x}C_{20}$ system.

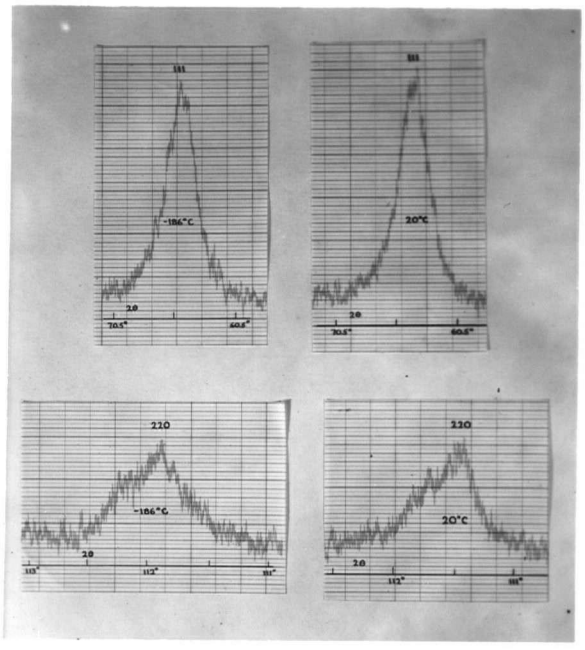

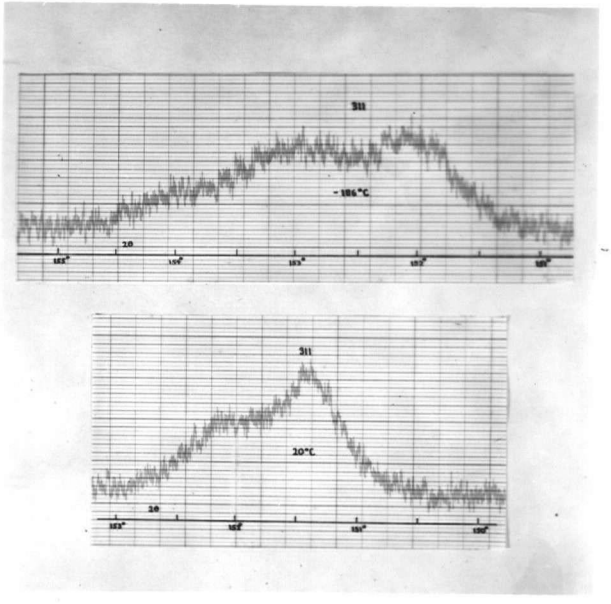

Figure 10 Comparison of X-ray intensity plots at -186°C and 20°C for a 2.85% Al alloy.

$Mn_{60}Ga_xZn_{20-x}C_{20}$ System

The variation of saturation magnetization with temperature for single phase alloys is shown in Figure 11. Alloys with gallium content greater than 6.63 atomic percent, which would be expected to show normal ferromagnetic behaviour, by analogy with $Mn_{60}Al_xZn_{20-x}C_{20}$ system, are not single phase unfortunately and hence cannot be considered. Alloys with gallium contents less than 6.63 atomic percent experience the same magnetic phenomena as in the aluminum system.

Saturation magnetization versus atomic percent gallium and Bohr magneton values versus atomic percent gallium were plotted and appear in Figures 12 and 13 respectively. The same interpretation of these graphs applies as that outlined in the $Mn_{60}Al_xZn_{20-x}C_{20}$ section. Transition temperatures for alloys of 0, 1.87 , and 3.79 atomic percent gallium are 231 ± 2, 210 ± 5, 185 ± 5°K respectively.

Curie temperatures were obtained from σ^2 vs. T plots. Values obtained are 415 ± 5°K for 1.87 percent gallium 390 ± 5°K for 3.79 percent gallium 380 ± 5°K for 6.63 percent gallium. Expected value for $Mn_{60}Zn_{20}C_{20}$ is 353 ± 5°K (no value obtainable for $Mn_{60}Ga_{20}C_{20}$). The values were not plotted as it is felt that it would be of little use since no simple relationship appears to exist between composition and Curie temperature for these alloys just as for the alloys in the aluminum system.

Single phase alloys exist only up to gallium concentration of 6.63 atomic percent. In this region X-ray Debeye-Sherrer powder photographs show lines characteristic of a face-centered cubic and also superlattice lines. Lattice parameters for these single phase alloys are plotted versus gallium content in Figure 14. Beyond 6.63 percent gallium another face-centered cubic phase appears along with the original face-centered cubic phase. The first or original phase disappears with even higher gallium contents and is replaced by a phase of unknown crystal structure which coexists with the second face-centered cubic phase.

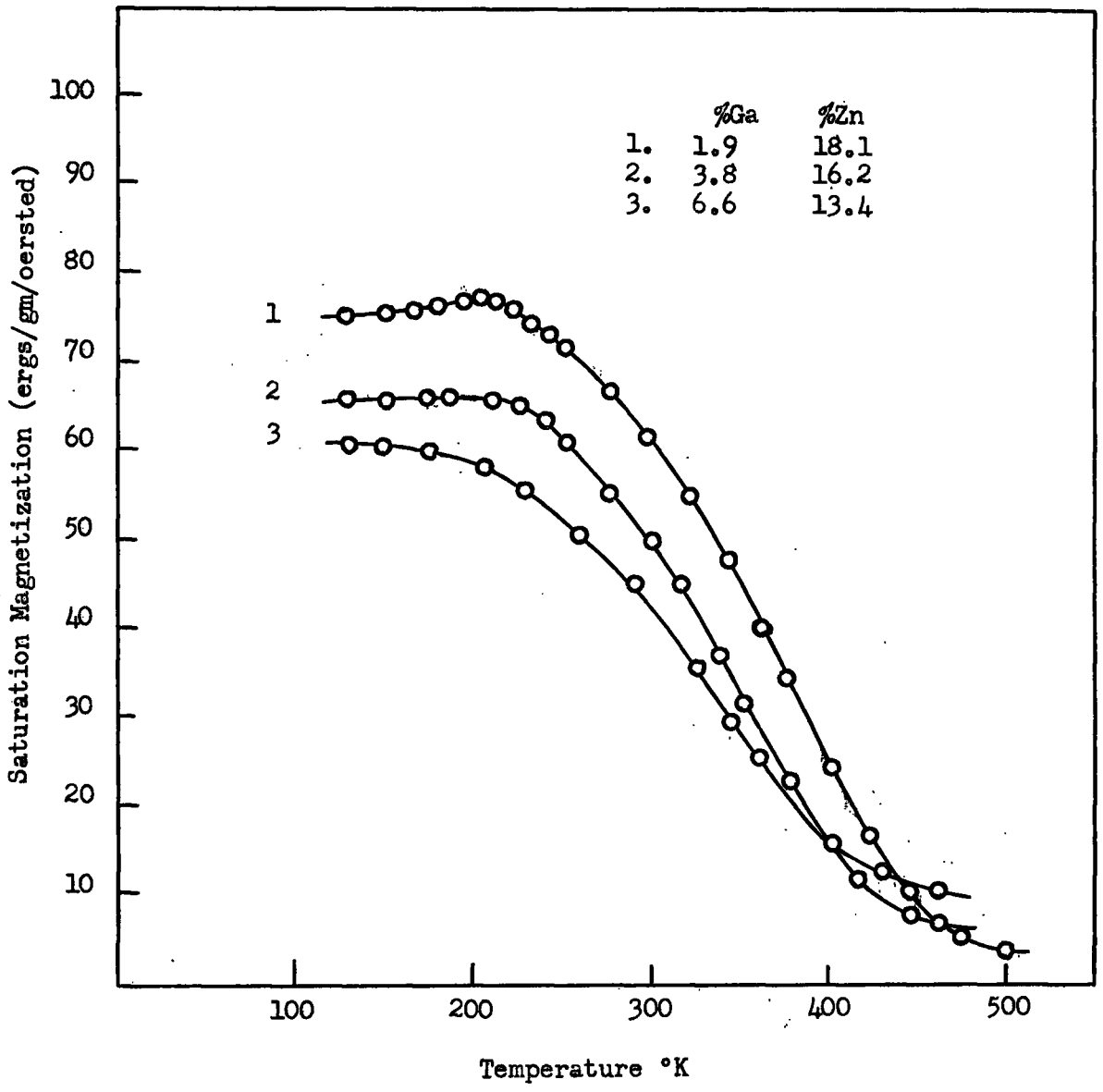

Figure 11 Variation of saturation magnetization with temperature for alloys in the $Mn_{60}Ga_xZn_{20-x}C_{20}$ system.

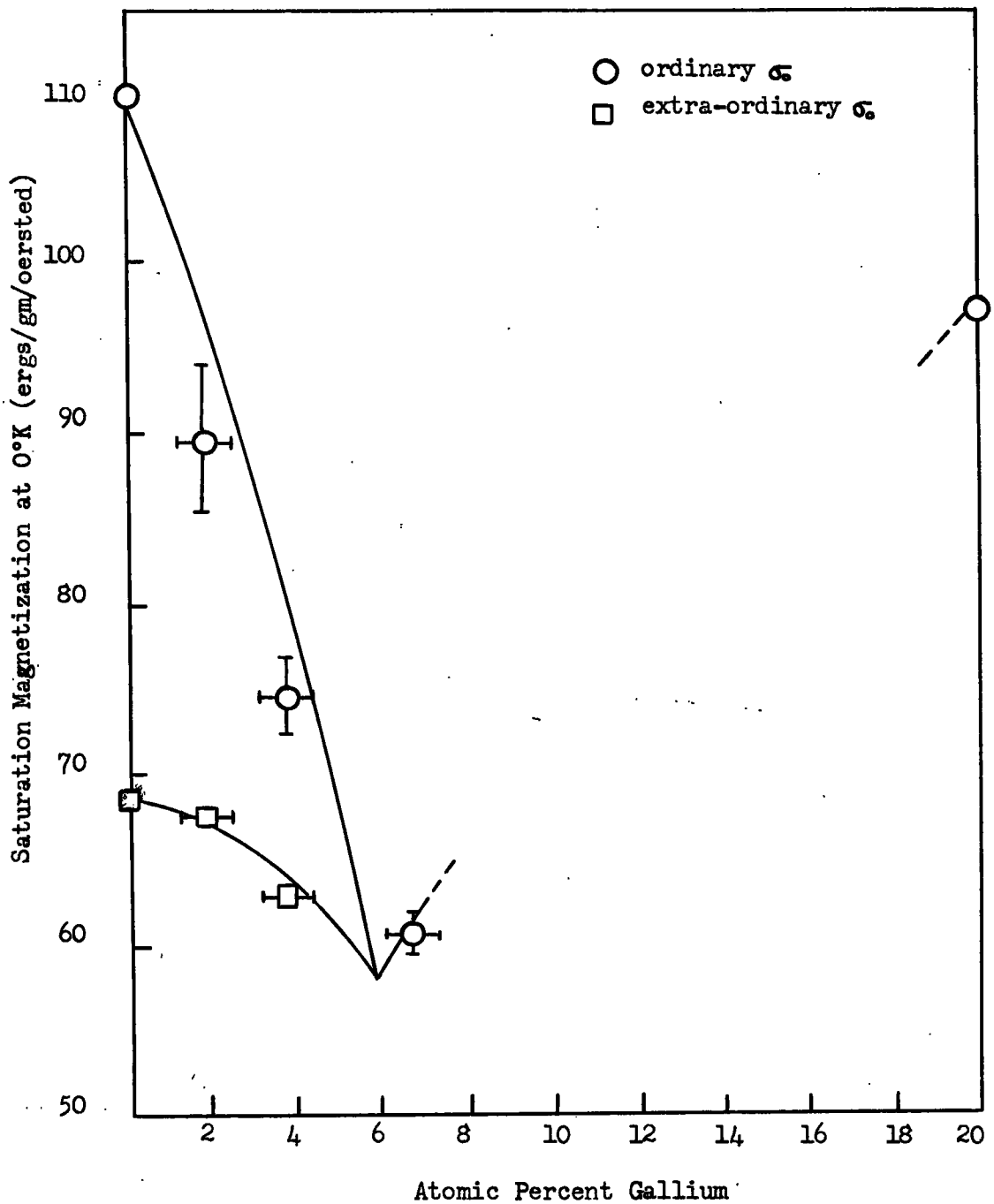

Figure 12 Variation of saturation magnetization with atomic percent gallium for alloys in the $Mn_{60}Ga_xZn_{20-x}C_{20}$ system.

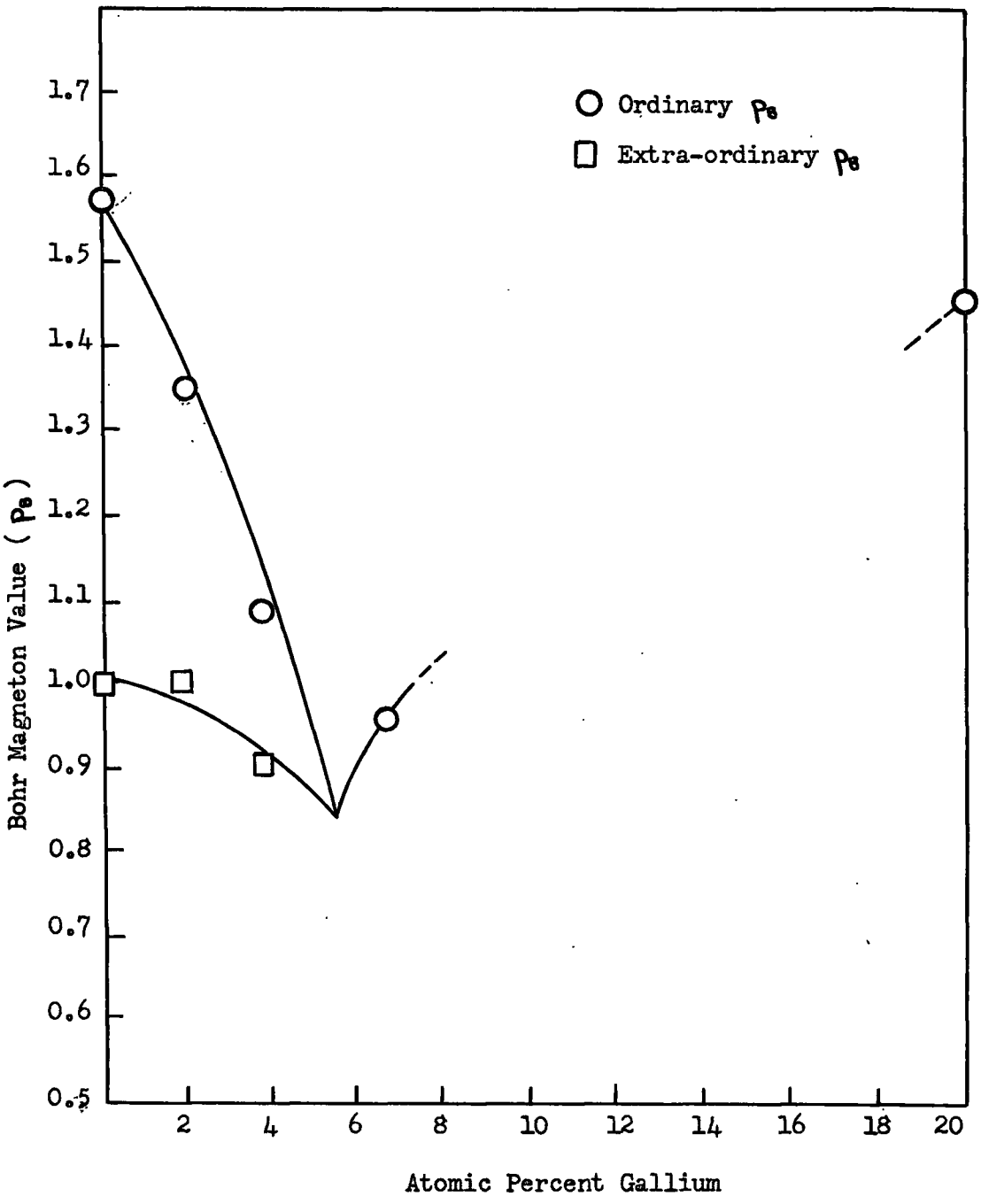

Figure 13 Bohr magneton value versus atomic percent gallium for the $Mn_{60}Ga_xZn_{20-x}C_{20}$ system.

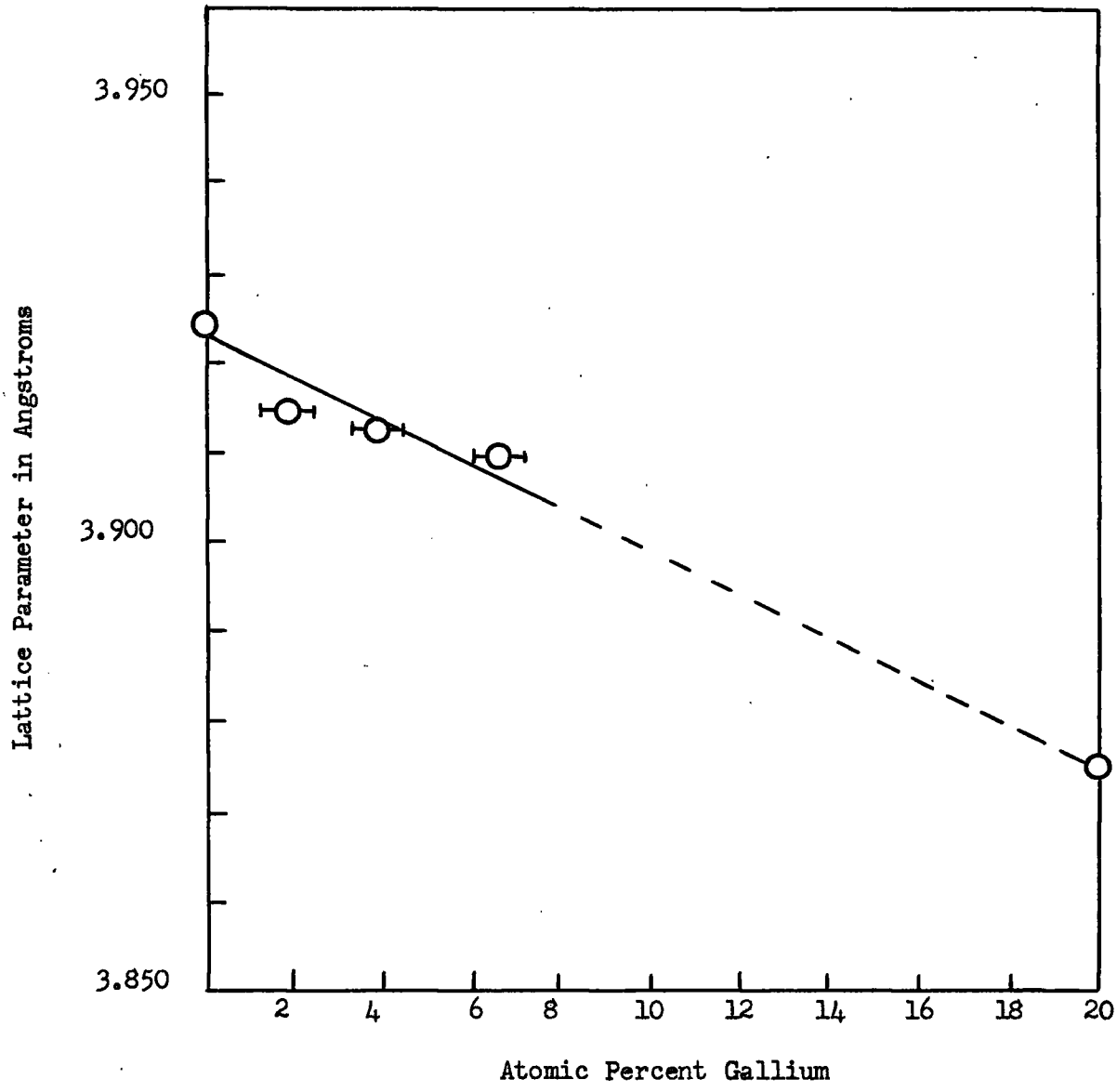

Figure 14 Variation of lattice parameter with atomic percent gallium for the $Mn_{60}Ga_xZn_{20-x}C_{20}$ system.

V. DISCUSSION OF RESULTS AND CONCLUSIONS

The assay results indicated that it was rather difficult to obtain alloys, in the $Mn_{60}Al_xZn_{20-x}C_{20}$ and $Mn_{60}Ga_xZn_{20-x}C_{20}$ systems, by sintering process, which had compositions same as those originally desired. However in most cases the final percentages of constituents were fairly close to the as-made-up compositions and in those cases where they were not the alloys were discarded. In order to make plotting of graphs and interpretation of results easier percentages of zinc and aluminum in $Mn_{60}Al_xZn_{20-x}C_{20}$ system were adjusted so that the aluminum plus zinc atomic percents totalled twenty, similarly for the gallium and zinc in the $Mn_{60}Ga_xZn_{20-x}C_{20}$ system. Manganese and carbon percentages may be considered as being essentially 60 and 20 atomic percent respectively as the assay results indicated that in most cases they were within one atomic percent of these figures. Variation to be expected in composition has been shown on graphs or accounted for in some manner and it is important to note that even though there is this slight variation in composition that the general trends as indicated in the graphs are unquestionably reliable.

Single phase alloys obtained in the $Mn_{60}Al_xZn_{20-x}C_{20}$ and $Mn_{60}Ga_xZn_{20-x}C_{20}$ systems were found to be highly-ordered structures as shown by Debeye-Sherrer powder photographs and inferred from structure determination for alloys close to the compositions $Mn_{60}Al_{20}C_{20}$ and $Mn_{60}Zn_{20}C_{20}$. In this highly-ordered structure manganese occupies face-center positions of cube, carbon occupies the body-center position, and aluminum, gallium or zinc atoms are at the cube corners. It is unfortunate that single phase alloys

could not be obtained over the complete range of compositions in the two systems.

Bohr magneton values expected for $Mn_{60}Al_{20}C_{20}$ and $Mn_{60}Zn_{20}C_{20}$ are 1.23 and 1.58 per manganese atom respectively. Since there are three manganese atoms per unit cell this would correspond to 3.69 and 4.74 Bohr magnetons per unit cell of $Mn_{60}Al_{20}C_{20}$ and $Mn_{60}Zn_{20}C_{20}$. The difference between the two values is of the order of 1 Bohr magneton and the difference between the valency of aluminum and zinc, which are corner atoms, is one. This would seem to suggest that the moment of the unit cell of this type of alloy is governed by the valency of the atom at the corner site. Hence we might expect the magnetic moment to decrease linearly as we go from $Mn_{60}Zn_{20}C_{20}$ to $Mn_{60}Al_{20}C_{20}$.

Consider now the Bohr magneton value expected for $Mn_{60}Ga_{20}C_{20}$ namely 1.43 Bohr magnetons per manganese atom or 4.29 Bohr magnetons per unit cell. Gallium has the same number of valence electrons as aluminum yet we obtain a different magnetic moment. Possible explanations of same are:

1. different interatomic distances
2. difference in total number of electrons.

Also if valency of the cube corner atom were governing factor we would once more expect a linear decrease in the magnetic moment as we go from $Mn_{60}Zn_{20}C_{20}$ to $Mn_{60}Ga_{20}C_{20}$.

The difference in interatomic distances in above alloy systems does not appear to be a governing factor as far as magnetic moment is concerned. Consider for example the plot of the expected parameter versus the expected Bohr mangeton value for $Mn_{60}Al_{20}C_{20}$, $Mn_{60}Zn_{20}C_{20}$ and $Mn_{60}Ga_{20}C_{20}$ as illustrated in Figure 15. If the parameter was a governing factor one would expect a linear relationship between the paramater and the Bohr

magneton value but such is certainly not the case.

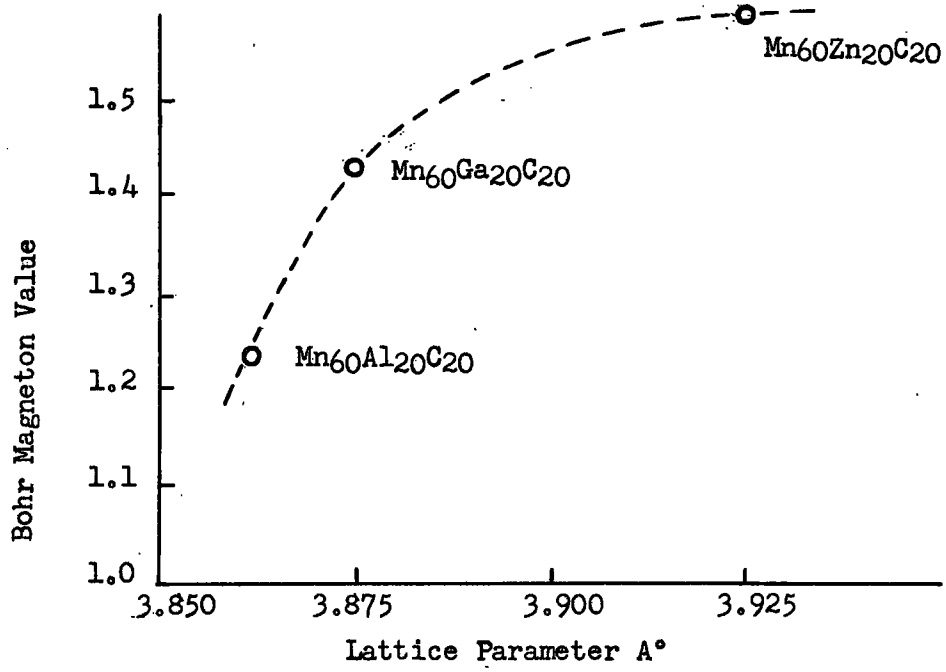

Figure 15 Variation of Bohr magneton value with lattice parameter for $Mn_{60}Al_{20}C_{20}$, $Mn_{60}Ga_{20}C_{20}$, and $Mn_{60}Zn_{20}C_{20}$.

Perhaps a look at the $Mn_{60}Al_xZn_{20-x}C_{20}$ system may serve to de-emphasize even further the role of the interatomic distance in affecting the magnetic moment. As the aluminum content is increased from 0 to 20 percent the magnetic moment decreases, reaching a minimum at approximately 5.5 percent, and then increases. The lattice parameter however decreases linearly over the same range. A fairly similar state of affairs is also found in the $Mn_{60}Ga_xZn_{20-x}C_{20}$ system as can be seen from the graphs in the results section. The variation of the lattice parameter with the magnetic moment as shown in the above two systems certainly appears to point to the fact that interatomic distance is not a governing factor in the alloy systems under discussion.

Returning once again to the variation of Bohr magneton value with atomic percent aluminum in the $Mn_{60}Al_xZn_{20-x}C_{20}$ system we note that the type of variation obtained (namely a decrease and then a increase in the Bohr magneton value) would seem to further rule out any simple valency mechanism. If a simple valency mechanism were operative we would expect a linear decrease in the Bohr magneton value when going from $Mn_{60}Zn_{20}C_{20}$ to $Mn_{60}Al_{20}C_{20}$. Even though single phase alloys are not available in the $Mn_{60}Ga_xZn_{20-x}C_{20}$ beyond 6.63 percent gallium it may be inferred from the results that the Bohr magneton value decreases with increasing gallium content up to 5.75 percent and then it should increase in some manner until it reaches the value expected for $Mn_{60}Ga_{20}C_{20}$. Once again we may conclude that a simple valency mechanism is not operative.

Intensity plots made with X-ray goniometer at 20°C and -186°C for an alloy of 2.85 atomic percent aluminum in the $Mn_{60}Al_xZn_{20-x}C_{20}$ system indicates that the original face-centered cubic structure observed at room temperature is slightly distorted becoming face-centered tetragonal at -186°C. This is similar to the transition mentioned earlier for an alloy near the composition $Mn_{60}Zn_{20}C_{20}$ in which case it was also noted that the transition in structure corresponded to a maximum in the saturation magnetization versus temperature curve. It therefore seems justifiable in assuming that, for alloys in the $Mn_{60}Al_xZn_{20-x}C_{20}$ and $Mn_{60}Ga_xZn_{20-x}C_{20}$ systems in which a maximum in the saturation magnetization occurs, a transition in structure occurs at a temperature corresponding to that at which the maximum appears.

However, the maximum in the saturation magnetization curve is not considered to be due to the transition in structure. In fact, if we

use the concept outlined earlier for the Mn-Zn-C system, whereby we have two opposing sublattices having different Curie points i.e. an ordering of manganese atoms, then it appears that the transition in structure is due to ordering of manganese atoms which occurs at a temperature corresponding to the maximum in the saturation magnetization curve.

No attempt will be made to try and explain the unexpected type of variation of Bohr magneton value with atomic percent aluminum or gallium in the $Mn_{60}Al_xZn_{20-x}C_{20}$ or $Mn_{60}Ga_xZn_{20-x}C_{20}$ systems. Similarly the mechanism operative in causing maximum in saturation magnetization curves will not be discussed further. We shall note that the magnetic anomaly appears to dissappear near an aluminum content of 5.5 atomic percent in $Mn_{60}Al_xZn_{20-x}C_{20}$ system and near a gallium content of 5.75 atomic percent in $Mn_{60}Ga_xZn_{20-x}C_{20}$ system. Considering the transition temperatures in the alloys possessing an anomaly in saturation magnetization plot, it is found that the transition temperature decreases with increasing aluminum or gallium thus indicating that it requires a lower temperature for ordering of the manganese atoms to occur.

It is felt that in order to try and explain magnetic properties of above systems that one would have to take into account such items as total number of electrons and exchange forces between these electrons. Such a study would be rather difficult and is beyond the scope of this investigation.

VI. BIBLIOGRAPHY

1. F. Brailsford, Magnetic Materials (1951) 29.

2. R.G. Butters, H.P. Myers, Philosophical Magazine, (1955), 46, 895.

3. R.G. Butters, H.P. Myers, Philosophical Magazine, (1955), 46, 132.

4. L. Néel, Annales de Physique, (1948), 3, 137.